

THE SHAPE OF THE SUNSPOT CYCLE*

DAVID H. HATHAWAY, ROBERT M. WILSON, and EDWIN J. REICHMANN
Space Science Laboratory, NASA Marshall Space Flight Center, Huntsville, AL 35812, U.S.A.

(Received 12 April, 1993; in revised form 10 December, 1993)

Abstract. The temporal behavior of a sunspot cycle, as described by the International sunspot numbers, can be represented by a simple function with four parameters: starting time, amplitude, rise time, and asymmetry. Of these, the parameter that governs the asymmetry between the rise to maximum and the fall to minimum is found to vary little from cycle to cycle and can be fixed at a single value for all cycles. A close relationship is found between rise time and amplitude which allows for a representation of each cycle by a function containing only two parameters: the starting time and the amplitude. These parameters are determined for the previous 22 sunspot cycles and examined for any predictable behavior. A weak correlation is found between the amplitude of a cycle and the length of the previous cycle. This allows for an estimate of the amplitude accurate to within about 30% right at the start of the cycle. As the cycle progresses, the amplitude can be better determined to within 20% at 30 months and to within 10% at 42 months into the cycle, thereby providing a good prediction both for the timing and size of sunspot maximum and for the behavior of the remaining 7–12 years of the cycle.

1. Introduction

Analyses of historical data on sunspots and related solar activity have revealed a wealth of information about the sunspot cycle. The well-known 11-year period associated with sunspot cycles was first reported by Wolf (1852) from his examination of the Zürich Observatory sunspot records. Earlier, Schwabe had announced an apparent systematic fluctuation with a shorter period (see Meadows, 1970; Shove, 1983). Waldmeier (1935, 1939) noted the asymmetry between the rise to maximum and the fall to minimum as well as the importance of the amplitude in determining the shape and length of the cycle. Wilson (1988) provides a useful description of other relationships found by examining the historical records of previous sunspot cycles.

Of course the sunspot cycle is *not* strictly periodic. Cycles are observed to vary both in size and length, and periods of inactivity like the Maunder minimum (Maunder, 1922; Eddy, 1976) are known to have occurred. Nonetheless, numerous authors have attempted to describe the cycle as a strictly periodic phenomenon with the hope of predicting future activity levels (see Wilson, 1984, and references cited therein).

Several authors have recently reported on efforts to describe the solar cycle in terms of smoothly varying functions with adjustable parameters. In particular, Nordemann (1992) fitted the rise to maximum and the decline to minimum with exponential functions requiring six free parameters (initial value, time-constant,

* The U.S. Government right to retain a non-exclusive, royalty free licence in and to any copyright is acknowledged.

and starting time for each phase) and Elling and Schwentek (1992) used a modified *F*-distribution density function that required five parameters.

Nordemann's analysis provides little in terms of true prediction for future cycle activity. Yearly averaged sunspot numbers are used so there are only 5–7 data points for each phase of the cycle and a good determination of the relevant parameters is not achieved until that phase is nearly complete. In addition, there seems to be little correlation between the parameters for the rising and declining phases and the cusp at maximum where the two phases meet is not at all representative of the true shape of the activity cycle. Such studies are valuable, however, in that they provide a time series of coefficients that describe individual solar cycles. (In a later paper by Nordemann and Trivedi (1992) the time sequence of these parameters is analyzed and some periodicities have been suggested.)

The approach taken by Elling and Schwentek (1992) is potentially more useful. Instead of using yearly means of sunspot numbers, they used quarterly (3-month) averages, fitting the entire cycle to a single function. They indicate the utility of using a fit to the *whole* cycle for help in forecasting future activity (such as maximum and minimum) for a given cycle. Their results also show that at least one of their parameters remains fixed for all of the cycles that they examined (cycles 10–21, the modern era of sunspot cycles; Wilson, 1992). This suggests that simpler functions with fewer parameters might be used to describe the shape of a sunspot cycle.

In this paper, we describe our efforts to find a simpler function that might be used to reproduce the shape of each sunspot cycle, simpler in terms of having fewer free parameters. We examine the relationships between the various parameters and assess the potential for an early determination of the relevant parameters for use in predicting future solar activity. The analysis reveals that, indeed, the temporal behavior of the sunspot number can be adequately described by a simple function of only *two* parameters for each cycle and that these parameters can be determined fairly early in the cycle.

2. The Sunspot Data and our Basis Function

For our analysis we use monthly averages of the International relative sunspot number (Waldmeier, 1961; McKinnon, 1987; updates published in *Solar Geophysical Data* available from NOAA/SEL, Boulder, Colorado). Although these data extend from 1749 to the present, some daily values for years prior to 1849 are missing, thereby making that data less reliable. These monthly averages are plotted in Figure 1 for the entire interval (1749–1992).

Inspection of Figure 1 reveals that individual cycles show a wide range of temporal behavior. For example, some cycles (like 12–16) are small in amplitude (about half the size of cycle 19), while others are considerably larger (like 18, 19, 21, and 22). Most cycles show substantial asymmetry, with the rise to maximum being faster than the fall to minimum. Further, smaller cycles tend to rise to maximum

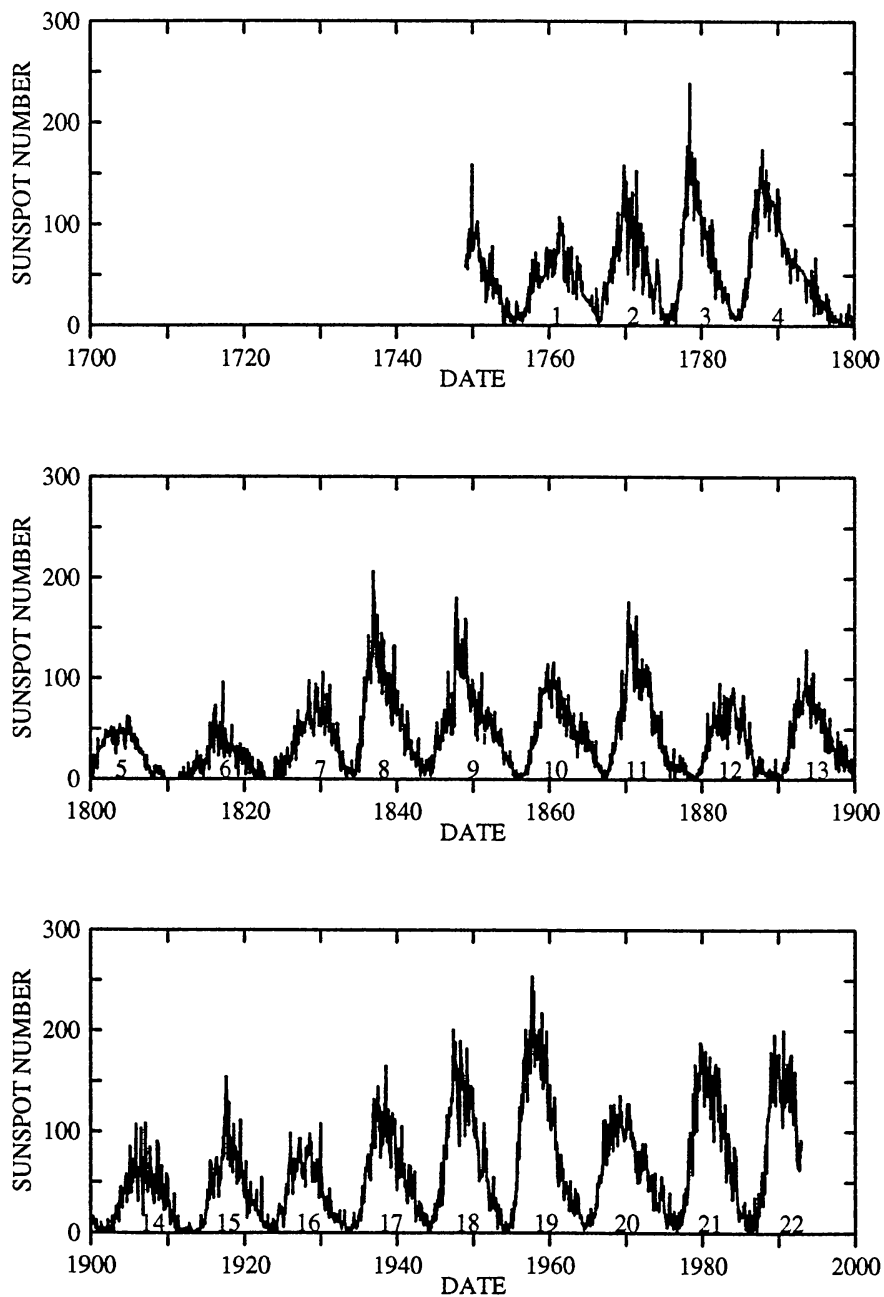


Fig. 1. Monthly averages of the International sunspot numbers for 1749 to 1992. This illustrates the cyclic behavior of the sunspot numbers and shows the variations in size and shape of each sunspot cycle.

more slowly than larger cycles (the Waldmeier effect). Lastly, while the average cycle length (minimum to minimum) is about 11 years, individual cycles vary in length from about 9 to 14 years. (Wilson (1987) has shown that the distribution of individual cycle lengths is better described using a bimodal distribution consisting of shorter and longer period cycles.)

We began our investigation by examining the rise toward maximum of sunspot number over the first two to three years of each cycle. We found that the rise can

be well represented by a function that increases as t^3 , where t is the time from the start of the cycle. Linear, quadratic, and exponential functions were, on average, poorer representations of this phase of the solar cycle. Similarly, we found that the decline of the sunspot cycle (from maximum to minimum) can be well represented by a function that decreases as $\exp(-t^2)$. Combining these results, we were led to investigate a function of the form

$$f(t) = a(t - t_0)^3 / \{\exp[(t - t_0)^2/b^2] - c\}, \quad (1)$$

where parameter a represents the amplitude and is directly related to the rate of rise from minimum; b is related to the time in months from minimum to maximum; c gives the asymmetry of the cycle; and t_0 denotes the starting time. This function reproduces both the rise and decay portions of the sunspot cycle and smoothly transitions between the portions at both minimum and maximum. It is similar to the Planck function but contains four free parameters and has a more rapid decline after maximum.

We determined the best-fit parameters for each cycle using the Levenberg–Marquardt method as described by Press *et al.* (1986). This method is a nonlinear least-squares fitting algorithm in which all four parameters can vary. The statistical errors in the monthly averages were taken to be the standard deviation in the average as determined from the daily values for 1849 to the present. We found that these errors are well represented by $s = 3.3\sqrt{R}$, where R is the monthly average sunspot number. By invoking this functional form we were able to represent the errors in the earlier less reliable era of sunspot measurements (before 1849).

Our estimates for the errors in the best-fit parameters were obtained by measuring their deviations from a series of 10^4 Monte-Carlo simulations for each cycle. These simulations used the best-fit parametric values to construct a basic time series. Each monthly value was then perturbed with normally-distributed random variations, using the standard deviations of the monthly averages as the standard deviation for the variations. Each simulation was then fit to the basis function and the best-fit parameters were then used to find the mean values and their variances.

3. Cycle Shape Parameters

In attempting to fit each cycle with the 4-parameter basis function we found that the process initially gave parameters with large uncertainties. Similarly good fits could be obtained by adjusting the starting time along with the other three parameters. However, if the starting time was fixed (at smoothed sunspot minimum for instance), the procedure was stabilized and well-determined values were obtained for the other parameters. The problem was then one of determining the *best* starting time for each cycle. Since the cycles are known to overlap by about 3 years, with new cycle spots appearing at high latitudes while old cycle spots are still seen at low latitudes (Brunner, 1943; Giovanelli, 1964), sunspot minimum is not necessarily the most appropriate starting time for a cycle.

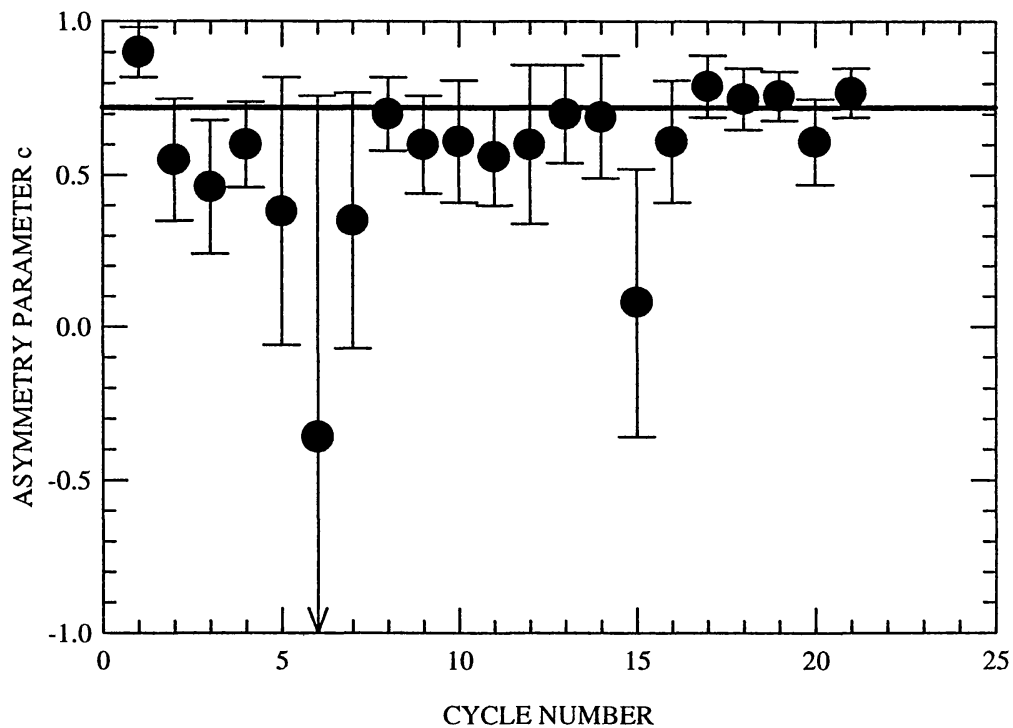


Fig. 2. Asymmetry parameter c and associated 2σ error bars for the functional fit to cycles 1–21. A single value, $c = 0.71$, is consistent with the best-fit values from all but three cycles and is shown by the thick horizontal line in the figure.

With the starting time set at sunspot minimum, our analysis showed that the symmetry parameter c could be fixed at a *constant* value for 21 complete cycles. Figure 2 depicts the measured values of c for each cycle with error bars that represent 2σ errors. Although variations do occur from cycle to cycle, they appear to be unrelated to the other parameters and the results are consistent with taking a single value of $c = 0.71$ for all cycles. This effectively reduces the number of parameters by one and also stabilizes the fitting procedure by removing one degree of freedom.

With $c = 0.71$ the time of maximum, t_{\max} , is given explicitly by

$$t_{\max} - t_0 = 1.081b \text{ months} , \quad (2)$$

where parameter b is also expressed in months. The value of the sunspot number at maximum, R_{\max} , is then given by

$$R_{\max} = 0.504ab^3 . \quad (3)$$

Examination of the best-fit parametric values for each cycle shows that parameters a and b are related. Cycles with large amplitudes (large a) take less time to rise to maximum (smaller values for b), the so-called the Waldmeier effect. We investigated functional fits to this relationship and noted that, for small a , parameter

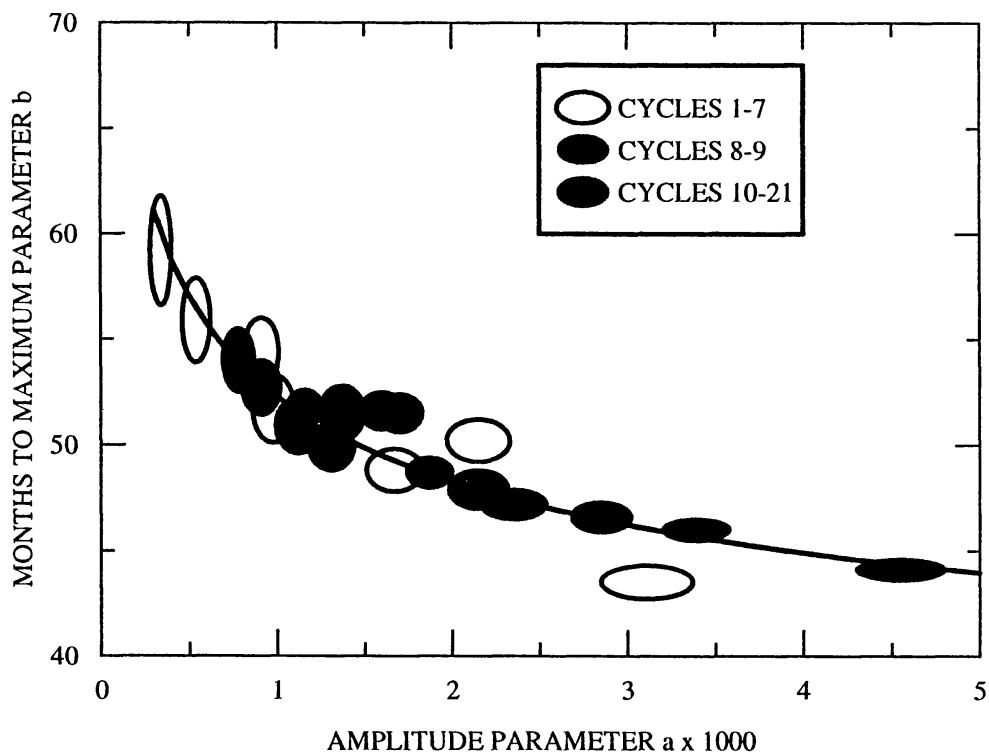


Fig. 3. Parameter b (months to maximum) plotted as a function of parameter a (amplitude) for cycles 1–21. This shows that small amplitude cycles rise to maximum more slowly than large amplitude cycles. Individual cycles are represented by 2σ error ellipses. The early, incomplete cycles are shown with open ellipses, the nearly complete cycles 8 and 9 as gray ellipses, and the recent cycles with fully-complete coverage as black ellipses. The functional fit given by (4) is represented by the thick line through the data.

b must be smaller than $a^{-1/3}$ for the maximum sunspot number, as given by (3), to decrease at small a as expected. Using $b(a) \sim a^{-1/4}$ and then fitting both t_0 and a for each cycle, we found a new set of starting times that differed slightly from that of minimum smoothed sunspot number. Using these values of t_0 still gives $c = 0.71$ and produces a much tighter fit for both $b(a)$ and for the functional fit to the sunspot data.

Figure 3 shows parameter b as a function of parameter a for all cycles using these optimized starting times. The ellipses represent 2σ errors, where black ellipses denote cycles 10–21 (the modern era), gray ellipses the less reliably known cycles 8 and 9 (still considered to be of ‘good’ quality), and open ellipses the earlier, poorly known cycles 1–7. A strong relationship between a and b is clearly seen, with cycles of large amplitude a rising more quickly to maximum as given by the smaller values for the parameter b . The best fit to this relationship is given by

$$b(a) = 27.12 + 25.15/(a \times 10^3)^{1/4} \quad (4)$$

which passes within 2σ of most (17 of 21) of the data points and is plotted as the thick line in Figure 3. A standard linear regression analysis between the best-fit b values and those obtained from (4) yields a linear correlation coefficient of

0.95 with a standard error of estimate equal to 1.4; the regression is found to be statistically significant at >99.9% level of confidence.

Setting $c = 0.71$ and using (4) to represent b in (1) gives a 2-parameter function for fitting to each sunspot cycle, with the parameters being the amplitude a and the starting time t_0 . The results of our analyses for these shape parameters are given in Table I. The first column gives the cycle number and the second through fourth columns give the results for the 3-parameter fit. The fifth column gives a measure of the goodness-of-fit as given by

$$\bar{\chi} = \sqrt{\left[\sum_{i=1}^N (R_i - f_i)^2 / s_i^2 \right] / N}, \quad (5)$$

where R_i is the monthly-averaged sunspot number, f_i is the functional fit value, s_i is the standard deviation for the monthly-averaged sunspot number, and N is the number of months in the cycle. A value for $\bar{\chi}$ of 1.0 indicates that, on average, the fitted function passes within one standard deviation of the data points. Columns 6–8 give the parameter values and $\bar{\chi}$ values for the 2-parameter fit to each cycle. The last column (9) gives $\bar{\chi}$ values for the 5-parameter fits of Elling and Schwentek (1992). (We did not calculate $\bar{\chi}$ values for Nordemann's fits because of the coarser time resolution from the use of yearly averages.)

The results shown in Table I indicate that, with the exception of cycles 5, 6, and 12, all three functions (the 3-parameter fit, the 2-parameter fit, and the 5-parameter fit of Elling and Schwentek) fit the data fairly well (typically within about 1σ of the data values). The 3-parameter function usually gives a slightly better fit than the 2-parameter function and both are usually better than the 5-parameter function of Elling and Schwentek (1992). (This is probably due to the use of quarterly averages by Elling and Schwentek.) These differences are not, however, considered significant. The more important result is that sunspot data can be adequately fit with a relatively simple function of only two parameters.

In Figure 4 we plot the monthly averages of the sunspot number along with our 2-parameter function for each cycle. The thin line in Figure 4 represents the data while the thick line is constructed using parameters from the 2-parameter fits given in Table I. This curve represents the sum of the contributions from both the current cycle at the date in question and from the previous cycle. While the contribution from the previous cycle becomes negligible well before the maximum of a cycle, it does tend to push the actual date of sunspot minimum ahead several months into the start of a new cycle. Figure 4 illustrates how well our 2-parameter function actually fits the data and shows our prediction for the remainder of this cycle.

4. Forecasting Potential

Our analysis suggests that the rote behavior of a sunspot cycle is governed by two parameters, starting time and amplitude. These parameters would be useful in

TABLE I
 Summary of best-fit parametric values for the three-parameter function, the two-parameter function, and goodness-of-fit parameter for the five-parameter function of Elling and Schwintek (1992, E and S).
 (Note: t_0 is our start date (year-month) for each cycle; it is not the traditional epoch of sunspot minimum.)

Cycle	Three-parameter fit			Two-parameter fit			E and S	
	$a \times 10^3$	b	t_0	$\bar{\chi}$	$a \times 10^3$	t_0	$\bar{\chi}$	$\bar{\chi}$
1	0.91 ± 0.05	54.4 ± 0.8	1755 – 11	0.71	1.01 ± 0.04	1755 – 11		0.75
2	1.67 ± 0.08	48.8 ± 0.6	1765 – 10	1.42	1.62 ± 0.06	1765 – 10		1.50
3	3.11 ± 0.13	43.5 ± 0.4	1775 – 03	1.70	2.35 ± 0.07	1775 – 03		1.56
4	2.15 ± 0.09	50.2 ± 0.5	1784 – 07	0.89	2.72 ± 0.08	1784 – 07		0.95
5	0.54 ± 0.04	55.9 ± 1.0	1798 – 06	2.34	0.51 ± 0.03	1798 – 06		2.50
6	0.34 ± 0.03	59.2 ± 1.3	1811 – 06	1.90	0.33 ± 0.03	1811 – 06		2.14
7	0.98 ± 0.06	51.7 ± 0.8	1824 – 03	0.94	0.93 ± 0.04	1824 – 03		1.01
8	2.35 ± 0.10	47.2 ± 0.4	1833 – 07	0.96	2.28 ± 0.07	1833 – 07		0.99
9	1.60 ± 0.07	51.6 ± 0.5	1844 – 05	0.99	1.95 ± 0.06	1844 – 05		0.97
10	1.37 ± 0.07	51.5 ± 0.7	1856 – 02	0.74	1.52 ± 0.05	1856 – 02		0.76
11	2.15 ± 0.09	47.9 ± 0.5	1866 – 11	0.88	2.16 ± 0.07	1866 – 11		1.35
12	0.91 ± 0.06	52.7 ± 0.7	1878 – 05	2.08	0.90 ± 0.04	1878 – 05		2.17
13	1.16 ± 0.06	51.5 ± 0.6	1889 – 05	0.90	1.17 ± 0.05	1889 – 05		0.91
14	0.78 ± 0.05	54.0 ± 0.8	1901 – 08	1.11	0.78 ± 0.04	1901 – 08		1.12
15	1.31 ± 0.07	49.9 ± 0.6	1913 – 03	0.88	1.23 ± 0.05	1913 – 03		1.16
16	1.12 ± 0.07	50.9 ± 0.7	1923 – 02	0.89	1.06 ± 0.05	1923 – 02		0.89
17	1.87 ± 0.07	48.7 ± 0.4	1933 – 11	0.86	1.89 ± 0.05	1933 – 11		1.10
18	2.85 ± 0.09	46.6 ± 0.4	1944 – 03	1.05	2.89 ± 0.07	1944 – 03		1.27
19	4.55 ± 0.13	44.1 ± 0.3	1954 – 04	0.91	4.45 ± 0.09	1954 – 04		1.61
20	1.70 ± 0.07	51.5 ± 0.5	1964 – 11	0.87	2.12 ± 0.06	1964 – 11		0.66
21	3.39 ± 0.10	46.0 ± 0.3	1976 – 06	0.89	3.52 ± 0.08	1976 – 06		0.89
22	3.20 ± 0.14	46.0 ± 0.6	1986 – 03	1.05	3.21 ± 0.08	1986 – 03		1.06

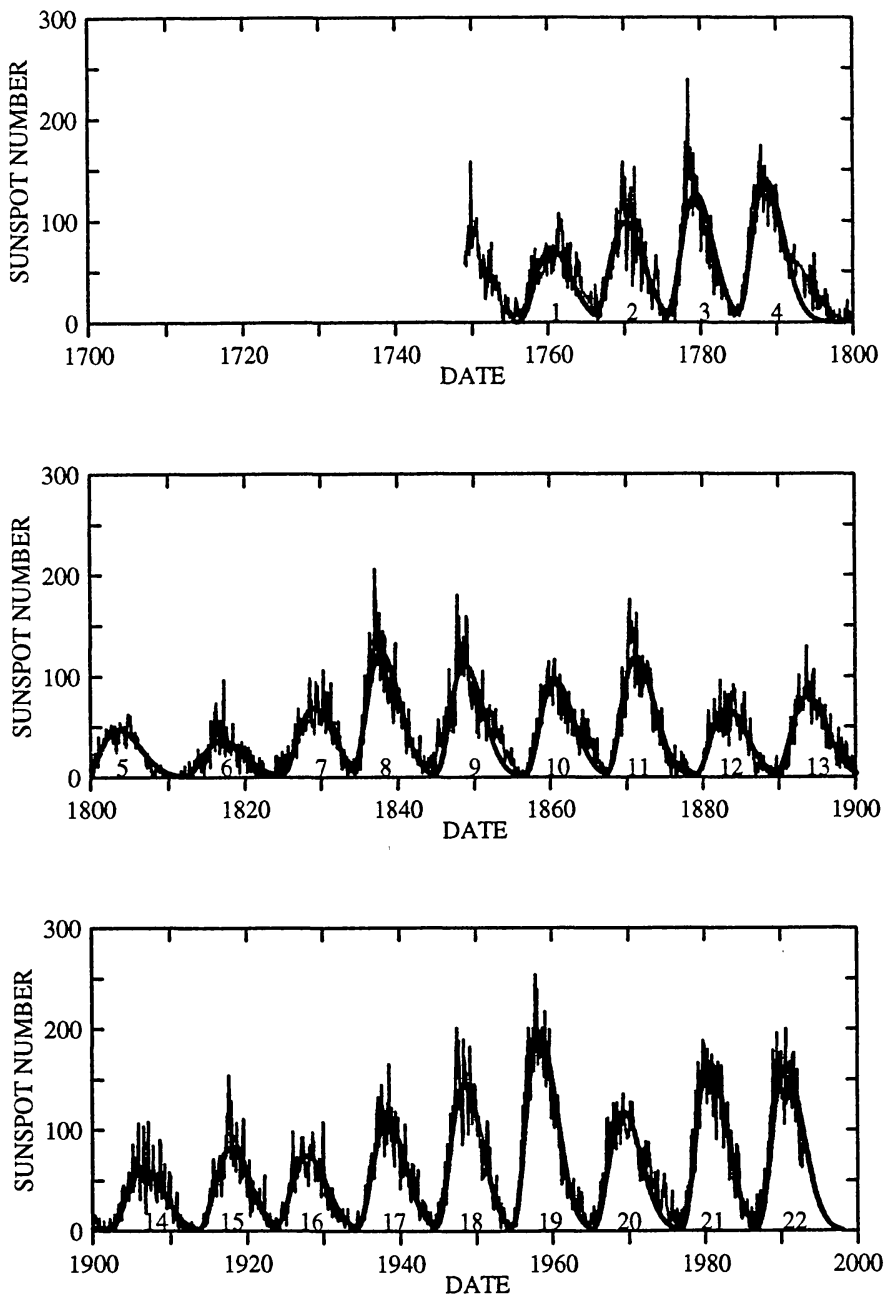


Fig. 4. A comparison of the sunspot data and our 2-parameter functional fit for the years 1749–1992 (cycles 1–22). The thin line represents the sunspot data. The thick line represents our 2-parameter fit for each cycle including our prediction for the remaining years of this cycle.

forecasting future activity if they could be determined early in the cycle or found to vary predictably from one cycle to the next. Given the starting time t_0 , an estimate of parameter a will then determine the behavior of the sunspot cycle over its full duration.

The value for parameter a , in fact, be quite accurately determined within the first 2–3 years following the start of the cycle. For the 21 completed cycles we determined best-fit values of parameter a using the 2-parameter function at a series

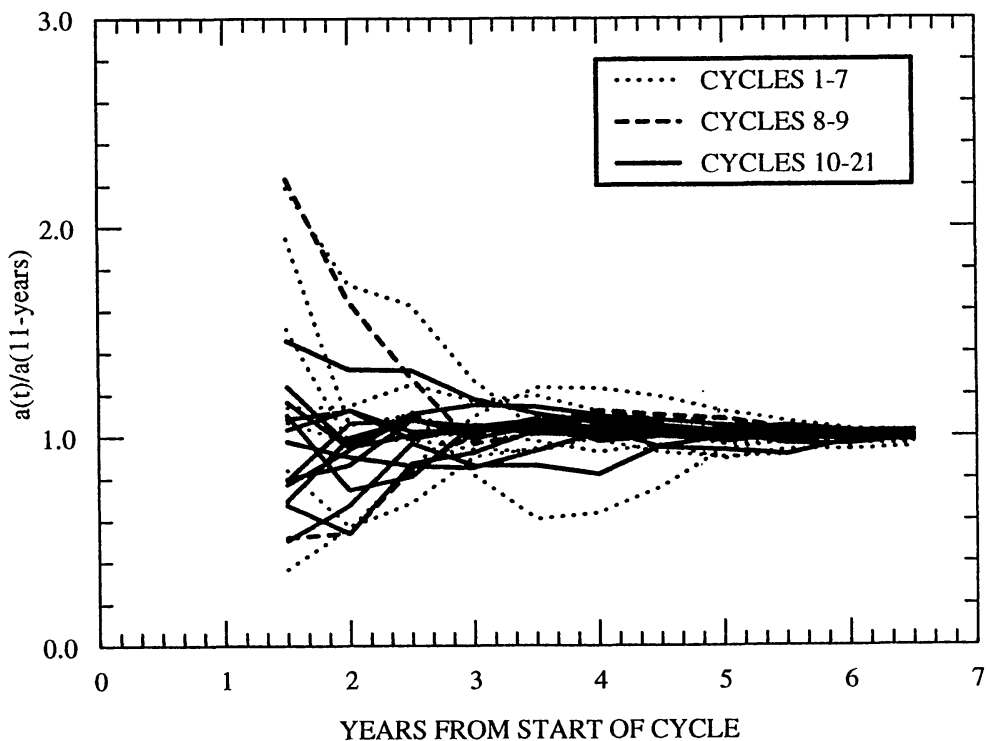


Fig. 5. Determinations of the amplitude parameter a at 6-month intervals into each cycle. The ratio of the estimated value of a to its final value determined at the end of the cycle is plotted for each cycle at 6-month intervals from 18 to 78 months. The modern cycles are represented with solid lines while the earlier, less reliable, cycles are represented by dotted and dashed lines. Although parameter a varies by a factor of 10 from cycle to cycle, it is determined to within 20% of its final value at 30 months and to within 10% at 42 months into the cycle.

of 6-month time intervals starting at 18 months into each cycle. The ratio of these values to the final values (determined at the end of each cycle) is plotted in Figure 5. The thick lines in Figure 5 represent the more recent (modern era) cycles for which we have complete coverage, while the broken lines represent the earlier cycles in which the observations were not taken every day. While the values for parameter a are found to vary by more than a factor of 10 from cycle to cycle (Table I), Figure 5 indicates that we can determine this parameter to within 20% of its final value at 30 months, and to within 10% of its final value at 42 months into the cycle. This suggests that fitting the behavior of the solar cycle by means of the 2-parameter function during the rising phase gives a prediction of the behavior of solar activity over the remaining 7 to 12 years of the cycle, including both the maximum phase and the decline to subsequent cycle minimum. (Similar predictability was found by Elling and Schwentek, 1992, with their 5-parameter function.)

Determining the amplitude and starting time of a cycle *before* it has started is a far more difficult problem. Examining the amplitude parameters for the last 22 cycles reveals a rather chaotic appearance. The mean value of a is 1.85×10^{-3} and there appears to be a slight upward trend in amplitudes over time with

$$a(n) = 9.2 \times 10^{-4} + 8.0 \times 10^{-5} n, \quad (6)$$

where n is the cycle number (1 to 22). A Fourier analysis of the amplitude parameters shows enhanced power at periods representing one cycle over the length of the dataset (always a suspicious result) as well as at periods of 7–8 cycles (the Gleissberg cycle) and at periods of 2–3 cycles (even-odd cycle behavior). Unfortunately, given the small number of cycles analyzed, it is difficult to determine the significance of any of these periodicities. We have, however, repeated the Fourier analysis on a series of 16 cycle samples (i.e., cycles 1–16, 2–17, etc.) and find that peaks at periods of 8 and 2 cycles *persist* until we start including the last four cycles (cycles 19–22). This difference in behavior for the most recent cycles might reflect a change in the Sun's magnetic dynamo. On the other hand it might reflect better observations of the Sun since the IGY in 1959. At present, we do not fully understand the significance of this finding.

An examination of the starting times for the last 22 cycles also suggests a rather chaotic behavior. The mean value for the length of the cycle, $[t_0(n+1) - t_0(n)]$, is 131.6 months and there appears to be a downward trend over time with

$$t_0(n+1) - t_0(n) = 134.9 - 0.30n \text{ months.} \quad (7)$$

This effect, combined with that given by (6), shows that the more recent cycles have been larger in amplitude and shorter in length than the earlier ones. We also find a weak correlation between the length of the cycle and the rise time as given by parameter b but the relationship is not better than (7) for predicting the length of a cycle. Both relationships give errors of several months to more than a year even during the modern era of sunspot observations.

Perhaps surprisingly, there does appear to be a weak inverse correlation between the amplitude of a cycle and the length of the *previous* cycle. Cycles that take a long time to get started tend to have small amplitudes. This is illustrated in Figure 6 where the data ellipses represent the amplitude of each cycle as functions of the length of the previous cycle. Here again the recent, high amplitude, cycles appear anomalous. Using cycles 2–18 we find that a linear fit with

$$a(n) = 6.57 \times 10^{-3} - 3.78 \times 10^{-5} [t_0(n) - t_0(n-1)] \quad (8)$$

characterizes the inferred relationship shown as the thick line in Figure 6. For most cycles this relationship gives an estimate for the amplitude of the cycle accurate to about 30% at the very beginning of the cycle. Using the average value for the amplitude is typically in error by about 75%, so our inferred relationship is definitely more useful than just taking the average. A standard linear regression on the predicted and observed amplitudes gives a correlation coefficient of 0.63, implying that about 40% of the variance in parameter is explained by the relationship.

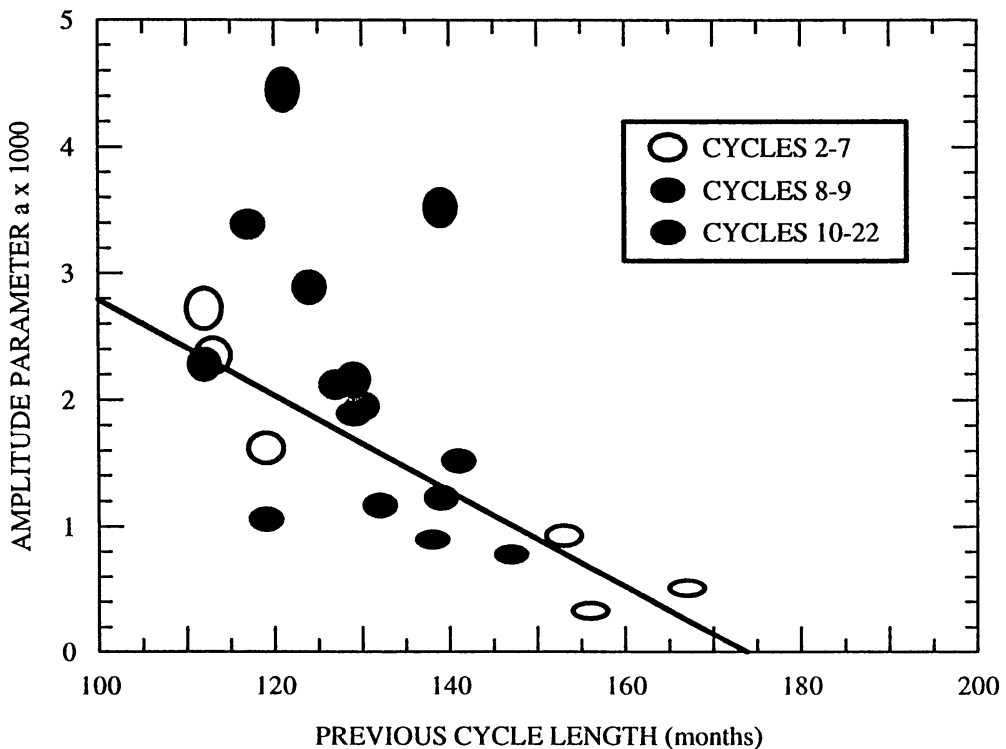


Fig. 6. Amplitude parameter a as a function of the length of the previous cycle. A weak correlation is inferred to exist between the two parameters suggesting that cycles that take longer to start tend to be smaller in amplitude. A linear fit to the values for cycles 2–18 is shown by the thick line through the data.

5. Conclusions and Discussion

Our study clearly shows that the shape of the sunspot cycle can be adequately described using a simple function with only two free parameters. This function was derived from a 4-parameter functional fit of the monthly mean sunspot numbers by fixing the asymmetry at a nominal value and expressing the time for the rise to maximum in terms of the amplitude of the cycle. While better fits might be obtained with more complicated functions containing more free parameters, the fact that the 2-parameter fit passes within about one standard deviation of the data points suggests that this function is adequate.

We have also found that the values of the amplitude parameter a are well determined early in the cycle. The length of the previous cycle can be used to estimate the amplitude of the following cycle to within about 30% at the start of the cycle, even though the actual amplitudes vary by more than a factor of 10 from cycle to cycle. By fitting sunspot numbers during the rising portion of the cycle using our 2-parameter function we found that we can reduce the uncertainty to about 20% at 30 months and to about 10% at 42 months into the cycle. This determination of the parameters provides an early estimate for the temporal behavior of the sunspot cycle over its remaining years *including* sunspot maximum.

One difficulty we found in fitting our function to the data was the determination

of the best starting time t_0 for each cycle. Although smoothed sunspot minimum gives a good estimate for these starting times, the optimal times were found *a posteriori* by fitting the full cycle with the 2-parameter function. For cycle 22, we fit the start of the cycle with the 3-parameter function and adjusted the starting time until parameters a and b agreed with (4). While this technique might also be used with other cycles, other datasets may also provide additional information for determining the best starting times. For example, the positions of sunspots have been reliably recorded since 1874. This information might be used to note the first appearance of high latitude spots. Further, magnetic polarity information has been available since 1917. Together these data might be used to better ascertain the best start time for a cycle.

Ideally, a theoretical model of the solar dynamo should provide the basis for observations of the physical processes on the Sun that are relevant to the workings of the dynamo itself. Observations of the rotation, magnetic field, and velocity field of the Sun would then provide the initial conditions for calculations of future solar activity levels. However, good working models of the solar dynamo have not as yet been developed. Furthermore, if the dynamo is concentrated at the base of the convection zone, the observations themselves may be difficult to obtain. Nonetheless, preliminary work in this direction shows some promise. Schatten *et al.* (1978) and Layden *et al.* (1991) have demonstrated that a determination of the polar magnetic field strength at sunspot minimum may provide a good indication for the strength of the following maximum. But this provides only a single value for the cycle and should be combined with a determination of the *shape* of the cycle to give a fuller description of solar activity levels. In lieu of a good theory and the relevant observations, we have relied on observations of the symptoms of the solar dynamo (i.e., sunspots) to look for characteristics that determine the shape and provide some additional predictive ability.

The procedures outlined here should also be applied to other data sets to examine any differences between the shape of the activity cycle as given by sunspot number and that given by quantities such as sunspot area, 10.7 cm flux, plage index, solar irradiance, etc. Such studies might then provide additional information which would help in forecasting future solar activity and in constraining models of the solar magnetic dynamo.

Acknowledgements

Support for this research was provided to Marshall Space Flight Center by the Solar Branch of NASA's Space Physics Division. The authors would also like to thank an anonymous referee for several useful comments on the content of this paper.

References

- Brunner, W.: 1943, *Publ. Zürich Obs.* **7**, 42.
- Eddy, J. A.: 1976, *Science* **192**, 1189.
- Elling, W. and Schwentek, H.: 1992, *Solar Phys.* **137**, 155.
- Giovanelli, R. G.: 1964, *The Observatory* **84**, 57.
- Layden, A. C., Fox, P. A., Howard, J. M., Sarajedini, A., Schatten, K. H., and Sofia, S.: 1991, *Solar Phys.* **132**, 1.
- Maunder, E. W.: 1922, *Brit. Astron. Assoc. J.* **32**, 140.
- McKinnon, J. A.: 1987, *Report UAG-95*, World Data Center A for Solar-Terrestrial Physics, Boulder, Colorado, 112 pp.
- Meadows, A. J.: 1970, *Early Solar Physics*, Pergamon Press, New York, p. 95
- Nordemann, D. J. R.: 1992, *Solar Phys.* **141**, 199.
- Nordemann, D. J. R. and Trivedi, N. B.: 1992, *Solar Phys.* **142**, 411.
- Press, W. H., Flannery, B. P., Teukolsky, S. A., and Vetterling, W. T.: 1986, *Numerical Recipes*, Cambridge University Press, Cambridge, 818 pp.
- Schatten, K. H., Scherrer, P. H., Svalgaard, L., and Wilcox, J. M.: 1978, *Geophys. Res. Letters* **5**, 411.
- Shove, D. J.: 1983, *Sunspot Cycles*, Hutchinson Ross Publ., Stroudsberg, Pennsylvania, p. 81.
- Waldmeier, M.: 1935, *Astron. Mitt. Zürich* **14** (No. 133), 105.
- Waldmeier, M.: 1939, *Astron. Mitt. Zürich* **14** (No. 138), 470.
- Waldmeier, W.: 1961, *The Sunspot Activity in the Years 1610–1960*, Schulthess and Co., Zürich, 171 pp.
- Wilson, R. M.: 1984, *NASA TM 86458*, Huntsville, Alabama, 43 pp.
- Wilson, R. M.: 1987, *J. Geophys. Res.* **92**(A9), 10101.
- Wilson, R. M.: 1988, *J. Geophys. Res.* **93**(A9), 10011.
- Wilson, R. M.: 1992, *Solar Phys.* **140**, 181.
- Wolf, R.: 1852, *Acad. Sci. Compt. Rend.* **35**, 704.